



As shown in Figure 1. for geometry relationship diagram of single-arm pantograph's movement component, the essence of which is a complex structure of four-bar linkage. The BE of figure is lower arm, which is the active rod and its angle is  $\hat{\alpha}$ . The AC is follower lever, its angle is  $\acute{\alpha}$ . Upper arm rod CDF directly contact with the head of pantograph. The  $\hat{\epsilon}$  that is between CD rod and vertical direction can be indirectly shown the height of pantograph's head. With the increase of  $\hat{\epsilon}$ , the height of pantograph's head can increases.

As shown in Table 1. for optimization variables and their meanings, the variable name derives from Figure 1. The optimization of pantograph's structural parameters is to seek the best combination of these design variables so that the pantograph's performance more superior.

**Table 1.** Design variables and meaning.

|                |   |
|----------------|---|
| a              | The vertical distance of AB                   |
| b              | The length of the CD                          |
| d              | The length of the DE                          |
| k              | The longitudinal distance of AB               |
| $\hat{\alpha}$ | The angle of the upper and lower on the frame |
| $L_{1-5}$      | The length of the AB/AC/DF/BE/CE              |

$$W_2 = \left[ \frac{L_2 \cos(\alpha) \tan(90 + \theta - \psi) + L_2 \sin(\alpha) + L_1 \cos(\delta) \tan(90 + \theta - \psi) - L_1 \sin(\delta)}{L_2 \cos(\alpha) \tan(90 + \theta - \psi) + L_2 \sin(\alpha)} \right] W_4 \quad (3)$$

$$W_3 = \left[ \frac{a + k \tan(\alpha) - L_4 \cos(\beta) \tan(\alpha) + L_4 \sin(\beta)}{L_4 \cos(\beta) \tan(\alpha) - L_4 \sin(\beta)} \right] W_4 \quad (4)$$

Among, the  $W_2$  is the speed of pull arm AC, and the  $W_3$  is the speed of upper arm rod CDF. The  $\hat{\alpha}$  is angle that is between ligature of fixed hinge bracket and X axis, and the  $\theta$  is angle that is between link CD and link CE.

(4) Equivalent Mass Calculation:

The equivalent mass of pantograph refers to the actual quality of the whole activities section of pantograph (e.g., skateboarding, bracket, framework, etc.) is calculated to the contact point of pantograph-catenary, which makes the whole pantograph has the quality with the same acceleration of the pantograph slide. Kinetic energy formula of pantograph components is as follows:

$$\begin{cases} T_{AC} = \frac{1}{2} I_2 W_2^2 \\ T_{BE} = \frac{1}{2} I_4 W_4^2 \\ T_{CDF} = \frac{1}{2} I_{CDF} W_3^2 + \frac{1}{2} M_{CDF} V_{CDF}^2 \end{cases} \quad (5)$$

Among, the  $I_2$  is the rotational inertia of pull arm AC, and the  $I_4$  is the rotational inertia of lower arm BE. The  $I_{CDF}$  is the rotational inertia of upper arm rod CDF, and the  $V_{CDF}$  is the speed of upper arm rod CDF, and the  $M_{CDF}$  is the total mass of upper arm rod CDF[7,8]. Based on the definition of

**2.2. Analysis and Research of Mathematical Model**

As shown in Figure 1., the A point is taken as the origin of coordinates, and the horizontal and vertical are taken as X and Y axes respectively. Based on the geometric diagram, using the geometry and plane four-bar linkage principle can gets the following relations.

(1) F point trajectory equation:

$$\begin{aligned} y &= L_3 \sin(\gamma + \theta - 90) + b \cos(\theta) + L_2 \sin(\alpha) \\ x &= L_3 \cos(\gamma + \theta - 90) - b \sin(\theta) - L_2 \cos(\alpha) \end{aligned} \quad (1)$$

(2) Institutions geometric relationships:

$$\begin{aligned} L_4 \sin(\beta) + a &= d \sin(\gamma + \theta - 90) + b \cos(\theta) + L_2 \sin(\alpha) \\ k + b \sin(\theta) + L_2 \cos(\alpha) &= d \cos(\gamma + \theta - 90) + L_4 \cos(\beta) \end{aligned} \quad (2)$$

(3) The speed relations between these links:

According to plane four-bar linkage principle, the length of each link can be confirmed approximately, whose result is  $L_4 > L_2 > L_1 > L_5$ . Combining the figure of four-bar linkage and the instantaneous center method can obtain speed relation of the each link[5,6]. If the speed of lower arm BE is  $W_4$ , through drawing the speed of pull arm AC and upper arm rod CDF can be calculated. The formula is as follows:

equivalent mass, the formula of equivalent mass is as follows:

$$\begin{aligned} T_{kinetic-energy} &= T_{AC} + T_{BE} + T_{CDF} \\ M_{equivalent-mass} &= \frac{2T_{kinetic-energy}}{V_F^2} \end{aligned} \quad (6)$$

Because the F point trajectory has already been calculated, the speed of the point F can be obtained by trajectory equation derivation, formula is:

$$M_{equivalent-mass} = \frac{I_2 W_2^2 + I_4 W_4^2 + I_{CDF} W_3^2 + M_{CDF} V_{CDF}^2}{(X'^2 + Y'^2)} \quad (7)$$

**3. Geometrical Parameters Optimization of Pantograph**

**3.1. Constraint Conditions and Optimization Targets of Mathematical Model**

**3.1.1. The Constraint Conditions**

In order to ensure the good running of high-speed pantograph, it must satisfy many requirements in the process of work.

- (1) The biggest rise height of pantograph's head is about 3000mm.
- (2) The working range of pantograph's head is 360~2600mm.

(3) The fall height of pantograph is 280mm.

(4) The direction of pantograph's head movement is ensured as far as possible to do vertical movement in the process of rising and falling pantograph. So the trajectory of pantograph's head is a vertical straight line, and the permissible deviations must be less than 30mm within the scope of work.

(5) The time of rising pantograph is controlled within 6~10s, and the time of falling pantograph is less than 6s.

(6) In the process of the interaction between pantograph and catenary, the excellent following performance of pantograph is required, so that the equivalent mass of pantograph should be as small as possible. Within the scope of the normal stiffness and strength, equivalent mass should be the least.

(7) When the pantograph's head in the highest position, the angle of rising pantograph is controlled within the range of 45~60

(8) From stability and operability, the relationship of each link is  $L_4 > L_2$  and  $L_1 > L_5$ .

The fourth among the above requirement is the optimization goal of pantograph's head trajectory, and the sixth is the optimization target of equivalent mass, and others are constraint conditions. From the previous formula, the trajectories of rising pantograph and equivalent mass are

$$M_{equivalent-mass} = \frac{M_2 L_2^2 W_2^2 + M_4 L_4^2 W_4^2 + 3I_{CDF} W_3^2 + 3M_3 V_{CDF}^2}{3[W_3 L_3 \sin(\gamma + W_3 t) - b W_3 \sin(W_3 t) + W_2 L_2 \cos(W_2 t)]^2} \quad (9)$$

Among,  $M_2$ ,  $M_4$  and  $M_3$ , respectively is the quality of the pull arm AC, lower arm BE and upper arm rod CDF.

### 3.2. MATLAB Optimization Method

According to the constraint conditions, each design variable is geometric parameters of planar mechanism, so it must meets the requirements of planar mechanism freedom movement and at the same time the basic requirements of pantograph work. Scope of every design variable which can be concluded as follows:

Table 2. The range of design variable values.

|   |
|---|
| $2200\text{mm} \leq L_3 \leq 2450\text{mm}$ |
| $1800\text{mm} \leq L_4 \leq 2000\text{mm}$ |
| $1150\text{mm} \leq L_2 \leq 1300\text{mm}$ |
| $900\text{mm} \leq k \leq 1100\text{mm}$    |
| $280\text{mm} \leq d \leq 400\text{mm}$     |
| $55\text{mm} \leq a \leq 80\text{mm}$       |
| $55\text{mm} \leq b \leq 80\text{mm}$       |
| $91.7^\circ \leq \alpha \leq 94.5^\circ$    |

This article is from the pantograph structure parameters to study the equivalent mass, so the formula of equivalent mass can be further simplified as:

decided by the design variables. So this is a multi-objective optimization problem [9,10].

### 3.1.2. The Objective Function

Multi-objective optimization problem has lots of solutions. The paper involves two optimization objectives, including trajectory is a vertical straight line. The x of trajectory equation is set as constant, as a constraint condition. This multi-objective problem is transformed into single objective problem, namely, under the same condition, how the parameters of the composite can make smaller reduction quality.

The x abscissa of point F is fixed value N, namely a formula:

$$x = L_3 \cos(\gamma + \theta - 90) - b \sin(\theta) - L_2 \cos(\alpha) = N$$

$$\cos(\alpha) = \frac{L_3 \cos(\gamma + \theta - 90) - b \sin(\theta) - N}{L_2} \quad (8)$$

The formula of angle is used as constraint conditions, and the value N is used as design variables.

According to the geometric relations of four bar linkage, the inertia formula of moment and the above a series of constraint conditions, further calculation analysis pantograph equivalent mass optimization objective function is:

$$M^* = \frac{L_2^2 W_2^2 + L_4^2 W_4^2 + 3I_{CDF} W_3^2 + 3V_{CDF}^2}{3[W_3 L_3 \sin(\gamma + W_3 t) - b W_3 \sin(W_3 t) + W_2 L_2 \cos(W_2 t)]^2} \quad (10)$$

In order to further obtain the optimal value of equivalent mass, combined with the budget law, again from the impact factors to consider, get the following formula:

$$M^{**} = \frac{(L_2 \cos(W_2 t) + L_1)^2 + L_4^2 + Q}{L_4^2 \sin^2(W_4 t) \cos^2(W_2 t) V_F^2} \quad (11)$$

$$Q = [(L_3 + b)^2 + (L_3 - b - d)^2][a + k \tan(W_2 t) - L_4 \sin(W_4 t)]^2$$

Combined with operation boundary condition, according to the above mathematical model, applying the optimization toolbox of MATLAB language programming, the optimization results are worked out. In which large values: d,  $L_4$ ,  $L_2$ ,  $\bar{a}$ , smaller values: a, b, k,  $L_3$ . Using MATLAB to further explore can obtain a set of optimal combination[11].

## 4. Optimization Results Simulation Verification

Pantograph dynamic model is built with ADAMS software, and the optimal solution is inputted to proceed dynamic simulation [12,13]. Optimization design requirement for pantograph limit height is 3000mm and the time of rising pantograph controls within 6s. The following is the simulation image of rising pantograph's height. (Note: the

simulation, the falling pantograph position in -800mm)

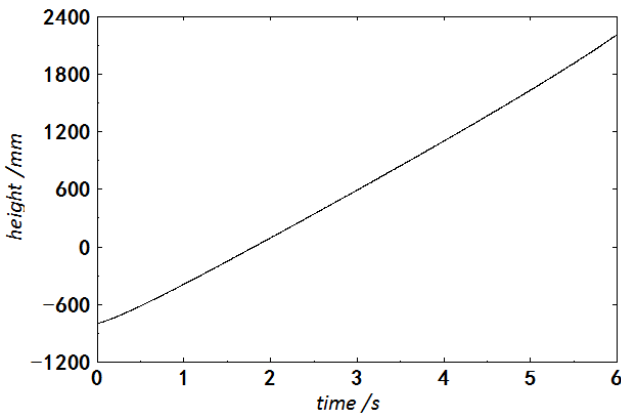


Figure 2. Rising height of pantograph.

The simulation image of rising pantograph’s trajectory is as follows. (Note: falling pantograph, pantograph’s head level in 2176mm)

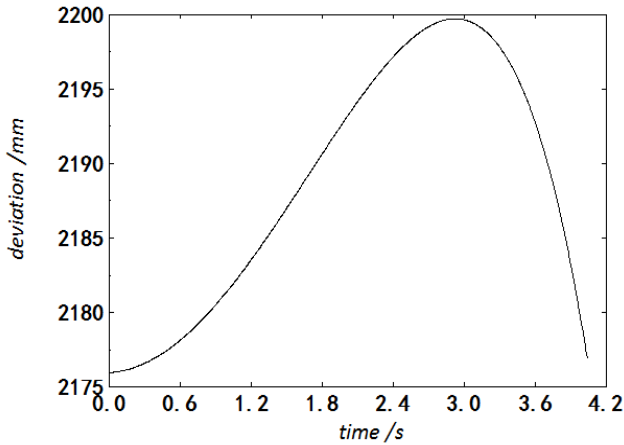


Figure 3. Rising deviation of pantograph.

Among them, the X-axis represents the running time of pantograph’s head, and Y-axis represents the running trajectory of pantograph’s head in the direction of the locomotive. By simulation image, the running trajectory of pantograph’s head is not a straight line. Ymin=2175mm, Ymax=2200mm, Ymax-Ymin=25mm. So in normal condition of pantograph, the trajectory deviation on the locomotive running direction is 25 mm < 30 mm, which conform to the requirements of the optimization design. Below image is curve relationship which is the running trajectory of pantograph’s head in the direction of the locomotive and rising pantograph’s height.

The figure shows that within the scope of the 25mm deviation, pantograph working range can be nearly 2500mm. For the present scope of pantograph’s work, this is satisfactory.

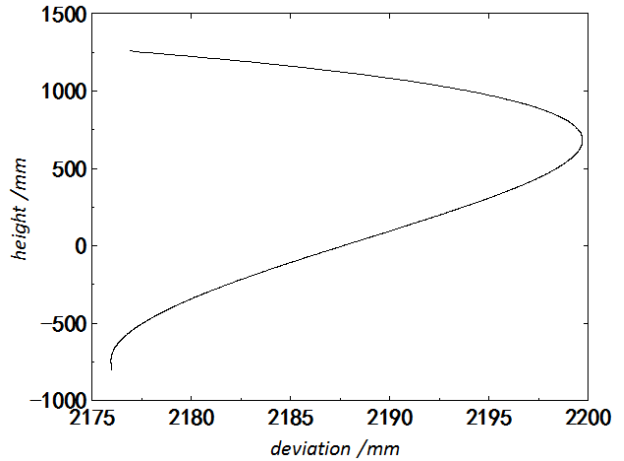


Figure 4. Trajectory of pantograph.

The equivalent mass do not direct simulate in the simulation software, so the pantograph’s vertical acceleration is used to indirectly reflect the following performance. Pantograph’s vertical acceleration simulation image is as follows.

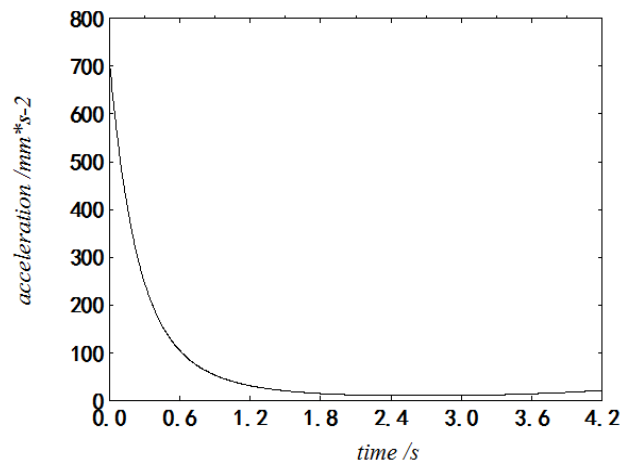


Figure 5. Vertical acceleration of pantograph.

Among them, the X-axis represents the pantograph’s running time, and Y-axis represents pantograph’s vertical acceleration. From the simulation image, first acceleration is bigger, within 1s, the acceleration drops rapidly. Within the scope of work, the vertical acceleration almost remains at a smaller value. So this is satisfactory.

## 5. Conclusions

The equivalent mass and rising pantograph’s trajectory are used as the optimization goals, so that will get single-arm pantograph structure parameters. Finally, these parameters are inputted into simulation software to verify. The verification results show that the pantograph will be risen within 6s, and the limit height of pantograph is 3000mm. The trajectory deviation from the vertical direction is 25mm within the scope of work 2500mm. Within the scope of work, pantograph’s vertical acceleration is small, so that following

performance is well. To illustrate that the structural parameters of the optimization design was conform to the requirements, have certain research significance.

## Acknowledgements

The paper is supported by innovation projects of postgraduate scientific research of Shanghai University of Engineering Science (number: A-0903-13-01129), the Twelfth Five-Year Program of Connotation Construction Project for Shanghai Local University (nhky-2014-07).

---

## References

- [1] Zhang Juan, Liu Zijian, Huang Daxiang, etc.. Low-speed single-arm pantograph structural parameters optimization design[J]. *Mechanical Research & Application*, 2004, 17(3):57-60.
- [2] Chen Mingguo, Xu Xiaoqin, Li Jun, etc.. Optimum Design and Verification of Geometric Parameters for Single-arm Metro Pantograph Structure[J]. *Urban Mass Transit*, 2009, 12(11):57-62.
- [3] Li Fengliang, Sun Yan, Su Qian. TSG3 Pantograph's Equivalent Mass[J]. *Journal of Railway*, 1998, 20(2):55-58.
- [4] Liu Zhaoyi. The modeling and simulation of pantograph-catenary coupled system on high-speed railway[D]. Changsha: Central South University, 2012.
- [5] Chen Xinbo, Lin Yan, etc.. Planar Four-bar Linkages With Double Crank Rotating The Driving Crank Two Turns in a Period of Motion[J]. *Chinese Journal of Mechanical Engineering*, 2003, 39(3):66-70.
- [6] Jong-Hwi Seo, Seok-Won Kim, Il-Ho Jung, et al. Dynamic analysis of a pantograph-catenary system using absolute nodal coordinates[J]. *Vehicle System Dynamics* 2006, 44(8): 615-630
- [7] Li Fengliang, Li Min, Tang Jianxiang. Establishment of the pantographs mechanical models and measurement of their parameters [J]. *Journal of Central South University (JCR-SCI)*, 2006, 37(1):194-199.
- [8] Mei Guiming, Zhang Weiping. Dynamics model and behavior of pantograph/catenary system[J]. *Journal of Traffic and Transportation Engineering*, 2002, 2(1):20-25.
- [9] Marian N. Velea, Per Wennhage, Dan Zenkert. Multi-objective optimization of vehicle bodies made of FRP sandwich structures[J]. *Composite Structures*, 2014, 111(5):75-84.
- [10] Marco Costa, Gian Marco Bianchi, Claudio Forte, et al. A numerical methodology for the multi-objective optimization of the DI diesel engine combustion[J]. *Energy Procedia*, 2014, 45(1):711-720.
- [11] Esmail Khorram, Keshavarz Khaledian, Mehrdad Khaledyan. A numerical method for constructing the Pareto front of multi-objective optimization problems [J]. *Journal of Computational and Applied Mathematics*, 2014, (261): 158-171
- [12] Jesus Peinado, Javier Ibanez, Ezack Arias, et al. Adams-bashforth and adams-moulton methods for solving differential Riccati equations[J]. *Computers and Mathematics with Applications*, 2010, 60(11):3032-3045.
- [13] Darina Hroncová, Michal Binda, Patrik Šarga, et al. Kinematical analysis of crank slider mechanism using MSC Adams/View[J]. *Procedia Engineering*, 2012, 48(9):213-222.